

# A note on the convergence of multigrid methods for the Riesz-space equation and an application to image deblurring

Danyal Ahmad<sup>a\*</sup>, Marco Donatelli<sup>a†</sup>, Mariarosa Mazza<sup>b‡</sup>, Stefano Serra-Capizzano<sup>a§</sup>,  
Ken Trotti<sup>c¶</sup>

<sup>a</sup> Dipartimento di Scienza e Alta Tecnologia, Università dell’Insubria, Como, Via Valleggio 11, 22100 Como, Italy

<sup>b</sup> Dipartimento di Matematica, Università degli studi di Roma Tor Vergata, Via della Ricerca Scientifica 1, 00133 Rome, Italy

<sup>c</sup> Facoltà di informatica, Università della Svizzera Italiana, Via Giuseppe Buffi 13, CH-6900 Lugano, Switzerland

## Abstract

In the past decades, a remarkable amount of research has been carried out regarding fast solvers for large linear systems resulting from various discretizations of fractional differential equations (FDEs). In the current work, we focus on multigrid methods for a Riesz-space FDE whose theoretical convergence analysis of such multigrids is currently limited to the two-grid method. Here we provide a detailed theoretical convergence study in the case of V-cycle and W-cycle. Moreover, we discuss its use combined with a band approximation and we compare the result with both  $\tau$  and circulant preconditionings. The numerical tests include 2D problems as well as the extension to the case of a Riesz-FDE with variable coefficients. Finally, we apply the best-performing method to an image deblurring problem with Tikhonov regularization.

## 1 Introduction

In the present work, we are interested in the fast numerical solution of special large linear systems stemming from the approximation of a Riesz fractional diffusion equation (RFDE). It is known that using standard finite difference schemes on equispaced gridding, in the presence of one-dimensional problems we end up with a dense real symmetric Toeplitz linear system, whose dense structure is inherited from the non-locality of the underlying symmetric operator. We study a one-dimensional RFDE discretized with a numerical scheme with precision order one mainly for the simplicity of the presentation. Nevertheless, the same analysis can be carried out either when using higher-order discretization schemes [1, 2] or when dealing with more complex higher-dimensional fractional models [3, 4].

---

\*dahmad@uninsubria.it (D. Ahmad)

†marco.donatelli@uninsubria.it (M. Donatelli)

‡mariarosa.mazza@uniroma2.it (M. Mazza)

§s.serracapizzano@uninsubria.it (S. Serra-Capizzano)

¶ken.trotti@usi.ch (K. Trotti)

While the matrix-vector product involving dense Toeplitz matrices has a cost of  $O(M \log M)$  with a moderate constant in the “big O” and with  $M$  being the matrix size, the solution can be of higher complexity in the presence of ill-conditioning. In connection with the last issue, it is worth recalling that the Toeplitz structure carries a lot of spectral information (see [5, 6] and references therein). As shown in [7, 2] the Euclidean conditioning of the coefficient matrices grows exactly as  $M^\alpha$ . Therefore the classical conjugate gradient (CG) method would need a number of iterations exactly proportional to  $M^{\alpha/2}$  to converge within a given precision.

In this perspective, a large number of preconditioning strategies for the preconditioned CG (PCG) have been proposed. One possibility is given by band-approximations of the coefficient matrices, which as discussed in [7, 8] does not ensure a convergence within a number of iterations independent of  $M$ , but still prove to be efficient for some values of the fractional order and whose cost stays linear within the matrix-size. As an alternative, the circulant proposal given in [9] has a cost proportional to the matrix-vector product and ensures convergence in the presence of 1D problems that do not include variable coefficients. Another algebraic preconditioner proven to be optimal consists in the  $\tau$  preconditioning explored in [10, 11]. In a multi-dimensional setting, the multilevel circulants are not well-suited [12], while the  $\tau$  preconditioning still shows optimal behavior. For other effective preconditioners, we refer the reader to [13] where the proposed preconditioner is based on a rational approximation of the Riesz operator.

Other approaches to the efficient solution of the ill-conditioned linear systems we are interested in include multigrid methods. Optimal multigrid proposals for fractional operators are given e.g. in [14, 15, 16, 8]. However, a theoretical convergence analysis of such multigrids is currently limited to the two-grid method. Here we provide a detailed theoretical convergence study in the case of V-cycle and W-cycle. Moreover, as multigrid methods are often applied as preconditioners themselves, and often to an approximation of the coefficient matrix instead of to the coefficient matrix itself, on the same line of what has been done in [8], we discuss a band approximation to be solved with a Galerkin approach which guarantees linear cost in  $M$  instead of  $O(M \log M)$  and that inherits the V-cycle optimality. We compare the resulting methods with both  $\tau$  and circulant preconditioning and apply the best performing strategy to an image deblurring problem with Tikhonov regularization.

The paper is organized as follows. In Section 2 we present the problem, the chosen numerical approximation, and the resulting linear systems. The main spectral features of the considered coefficient matrices are also recalled. In Section 3 we describe the essentials of multigrid methods and give the description of our proposal and its analysis, while in Section 4 we discuss its use applied to a band approximation of the coefficient matrix. Section 5 contains a wide set of numerical experiments that compare the multigrid with state-of-the-art preconditioners and include 2D problems as well as the extension to the case of an RFDE with variable coefficients. Section 6 is devoted to applying the best preconditioning strategy to an image deblurring problem. Future research directions and conclusions are given in Section 7.

## 2 Preliminaries

The current section briefly introduces the continuous problem, its numerical approximation scheme, and the resulting linear systems. The main spectral features of the considered coefficient matrices are recalled as well.

As anticipated in the introduction, we consider the following one-dimensional Riesz Fractional Diffusion Equation (1D-RFDE) given by

$$-d \frac{\partial^\alpha u(x)}{\partial |x|^\alpha} = m(x), \quad x \in \Omega = [a, b] \quad (2.1)$$

with boundary conditions

$$u(x) = 0, \quad x \in \partial\Omega, \quad (2.2)$$

where  $d > 0$  is the diffusion coefficient,  $m(x)$  is the source term, and  $\frac{\partial^\alpha u(x)}{\partial |x|^\alpha}$  is the 1D-Riesz fractional derivative for  $\alpha \in (1, 2)$ , defined as

$$\frac{\partial^\alpha u(x)}{\partial |x|^\alpha} = c(\alpha)({}_a D_x^\alpha u(x) + {}_x D_b^\alpha u(x)), \quad (2.3)$$

with  $c(\alpha) = -\frac{1}{2 \cos \frac{\alpha\pi}{2}} > 0$ , while  ${}_a D_x^\alpha u(x)$  and  ${}_x D_b^\alpha u(x)$  are the left and right Riemann-Liouville fractional derivatives.

For the approximation of the problem, we define the uniform space partition on the interval  $[a, b]$ , that is

$$x_i = a + ih, \quad h = \frac{b-a}{M+1}, \quad i = 1, \dots, M. \quad (2.4)$$

Here the left and right fractional derivatives in (2.3) are numerically approximated by the shifted Grünwald difference formula as

$$\begin{aligned} {}_a D_x^\alpha u(x_i) &= \frac{1}{h^\alpha} \sum_{k=0}^{i+1} g_k^{(\alpha)} u(x_{i-k+1}) + O(h), \\ {}_x D_b^\alpha u(x_i) &= \frac{1}{h^\alpha} \sum_{k=0}^{M-i+2} g_k^{(\alpha)} u(x_{i+k-1}) + O(h), \end{aligned} \quad (2.5)$$

with  $g_k^{(\alpha)}$  being the alternating fractional binomial coefficients, whose expression is

$$g_k^{(\alpha)} = (-1)^k \binom{\alpha}{k} = \frac{(-1)^k}{k!} \alpha(\alpha-1) \cdots (\alpha-k+1), \quad k \in \mathbb{N}_0. \quad (2.6)$$

By employing the approximation in (2.5) to equation in (2.1) and using (2.3) and (2.6), we obtain the required scheme as follows

$$-d \frac{c(\alpha)}{h^\alpha} \left( \sum_{k=0}^{i+1} g_k^{(\alpha)} u_{i-k+1} + \sum_{k=0}^{M-i+2} g_k^{(\alpha)} u_{i+k-1} \right) = m_i, \quad i = 1, \dots, M. \quad (2.7)$$

By defining  $\mathbf{u} = [u_1, u_2, \dots, u_M]^T$  and  $\mathbf{m} = [m_1, m_2, \dots, m_M]^T$ , the resulting approximation equations (2.7) can be written in matrix form as

$$\bar{c}(\mathcal{G}_M^\alpha + \mathcal{G}_M^{\alpha T}) \mathbf{u} = \mathbf{m}$$

and, by defining  $\mathbf{G}_M^{(\alpha)} = \mathcal{G}_M^\alpha + \mathcal{G}_M^{\alpha T}$ , we have

$$A_M^\alpha \mathbf{u} = \mathbf{m}, \quad (2.8)$$

with  $A_M^\alpha = \bar{c} \mathbf{G}_M^{(\alpha)}$ ,  $\bar{c} = -\frac{dc(\alpha)}{h^\alpha}$ , and

$$\mathcal{G}_M^\alpha = \begin{bmatrix} g_1^{(\alpha)} & g_0^{(\alpha)} & 0 & \cdots & 0 & 0 \\ g_2^{(\alpha)} & g_1^{(\alpha)} & g_0^{(\alpha)} & \cdots & 0 & 0 \\ \vdots & \ddots & \ddots & \ddots & \ddots & \vdots \\ \vdots & \ddots & \ddots & \ddots & \ddots & \vdots \\ g_{M-1}^{(\alpha)} & g_{M-2}^{(\alpha)} & \cdots & \cdots & g_1^{(\alpha)} & g_0^{(\alpha)} \\ g_M^{(\alpha)} & g_{M-1}^{(\alpha)} & \cdots & \cdots & g_2^{(\alpha)} & g_1^{(\alpha)} \end{bmatrix}_{M \times M} \quad (2.9)$$

being a lower Hessenberg Toeplitz matrix. The fractional binomial  $g_k^{(\alpha)}$  coefficients satisfy few properties summarised in the following Lemma 2.1 (see [3, 17, 18]).

**Lemma 2.1.** For  $1 < \alpha < 2$ , the coefficients  $g_k^{(\alpha)}$  defined in (2.6) satisfy

$$\begin{cases} g_0^{(\alpha)} = 1, & g_1^{(\alpha)} = -\alpha, & g_0^{(\alpha)} > g_2^{(\alpha)} > g_3^{(\alpha)} > \dots > 0, \\ \sum_{k=0}^{\infty} g_k^{(\alpha)} = 0, & \sum_{k=0}^n g_k^{(\alpha)} < 0, & \text{for } n \geq 1. \end{cases} \quad (2.10)$$

Using Lemma 2.1, it has been proven in [18] that the coefficient matrix  $A_M^\alpha$  is strictly diagonally dominant and hence invertible. To determine its generating function and study its spectral distribution, tools on Toeplitz matrices have been used (see [7]). A short review of these results follows.

**Definition 1.** [5] Given  $f \in L^1(-\pi, \pi)$  and its Fourier coefficients

$$a_k = \frac{1}{2\pi} \int_{-\pi}^{\pi} f(x) e^{-ikx} dx, \quad i^2 = -1, \quad k \in \mathbb{Z}, \quad (2.11)$$

we define  $T_M(f) \in \mathbb{C}^{M \times M}$  the Toeplitz matrix

$$T_M(f) = \begin{bmatrix} a_0 & a_{-1} & a_{-2} & \cdots & \cdots & a_{1-M} \\ a_1 & a_0 & a_{-1} & \cdots & \cdots & a_{2-M} \\ \vdots & \ddots & \ddots & \ddots & \ddots & \vdots \\ \vdots & \ddots & \ddots & \ddots & \ddots & \vdots \\ a_{M-2} & \ddots & \ddots & \ddots & \ddots & a_{-1} \\ a_{M-1} & a_{M-2} & \cdots & \cdots & a_1 & a_0 \end{bmatrix} \quad (2.12)$$

generated by  $f$ . In addition, the Toeplitz sequence  $\{T_M(f)\}_{M \in \mathbb{N}}$  is called the family of Toeplitz matrices generated by  $f$ .

For instance, the tridiagonal Toeplitz matrix

$$\mathcal{G}_M^2 = \begin{bmatrix} 2 & -1 & & & & \\ -1 & 2 & -1 & & & \\ & \ddots & \ddots & \ddots & & \\ & & -1 & 2 & -1 & \\ & & & -1 & 2 & \end{bmatrix}$$

associated with a finite difference discretization of the Laplacian operator is generated by

$$l(x) = 2 - 2 \cos(x). \quad (2.13)$$

Note that for Toeplitz matrices  $T_M(f)$ ,  $M \in \mathbb{N}$ , as in (2.12), to have a generating function associated to the whole Toeplitz sequence, we need that there exists  $f \in L^1(-\pi, \pi)$  for which the relationship (2.11) holds for every  $k \in \mathbb{Z}$ .

In the case where the partial Fourier sum

$$\sum_{k=-M+1}^{M-1} a_k e^{ikx}$$

converges in infinity norm,  $f$  coincides with its sum and is a continuous  $2\pi$  periodic function, given the Banach structure of this space equipped with the infinity norm. A sufficient condition is that  $\sum_{k=-\infty}^{\infty} |a_k| < \infty$ , i.e., the generating function belongs to the Wiener class, which is a closed sub-algebra of the continuous  $2\pi$  periodic functions.

Now, according to (2.9), we define

$$b_{M,\alpha}(x) = \sum_{k=0}^M g_k^{(\alpha)} e^{i(k-1)x}.$$

Hence the partial Fourier sum associated to  $\mathbf{G}_M^{(\alpha)}$  is

$$b_{M,\alpha}(x) + \overline{b_{M,\alpha}(x)} = 2 \sum_{k=0}^M g_k^{(\alpha)} \cos((k-1)x).$$

Fixed  $d = 1$ , from (2.9) it is evident that the matrix  $h^\alpha A_M^\alpha = c(\alpha) \mathbf{G}_M^{(\alpha)}$  is symmetric, Toeplitz, and is generated by the following real-valued even function on  $[-\pi, \pi]$ , defined in the following lemma.

**Lemma 2.2.** [19, 7] *The generating function of  $h^\alpha A_M^\alpha = c(\alpha) \mathbf{G}_M^{(\alpha)}$  is*

$$f_\alpha(x) = -c(\alpha) 2^{\alpha+1} \left( \sin \frac{x}{2} \right)^\alpha \cos \left( x \left( 1 - \frac{\alpha}{2} \right) + \frac{\alpha\pi}{2} \right), \quad x \in [0, \pi]. \quad (2.14)$$

- For  $\alpha = 2$ ,  $f_2(x) = l(x) = 2 - 2 \cos x$ .
- For  $\alpha = 1$ ,  $f_1(x) = \frac{1}{2}l(x)$

As observed in [7], the function  $f_\alpha(x)$  has a unique zero of order  $\alpha$  at  $x = 0$  for  $1 < \alpha \leq 2$ .

By using the extremal spectral properties of Toeplitz matrix sequences (see e.g. [20, 21, 22]) and by combining it with Lemma 2.2, for  $\alpha \in (1, 2)$ , the obtained spectral information can be summarized in the following items (see again [7]):

- any eigenvalue  $\lambda$  of  $h^\alpha A_M^\alpha$  belongs to the open interval  $(0, r)$  with  $0 = \min f_\alpha$ ,  $r = \max f_\alpha > 0$ ;
- $\lambda_{\max}(h^\alpha A_M^\alpha)$  is monotonic strictly increasing converging to  $r = \max f_\alpha$ , as  $M$  tends to infinity;
- $\lambda_{\min}(h^\alpha A_M^\alpha)$  is monotonic strictly decreasing converging to  $0 = \min f_\alpha$ , as  $M$  tends to infinity;
- by taking into account that the zero of the generating function  $f_\alpha$  has exactly order  $\alpha \in (1, 2]$ , it holds that

$$\lambda_{\min}(h^\alpha A_M^\alpha) \sim \frac{1}{M^\alpha},$$

where, for nonnegative sequences  $\alpha_n, \beta_n$ , the writing  $\alpha_n \sim \beta_n$  means that there exist real positive constants  $0 < c \leq C < \infty$ , independent of  $n$  such that  $c\alpha_n \leq \beta_n \leq C\alpha_n, \forall n \in \mathbb{N}$ .

As a consequence of the third and of the fourth items reported above, the Euclidean conditioning of  $h^\alpha A_M^\alpha$  grows exactly as  $M^\alpha$ .

Therefore, classical stationary methods fail to be optimal, in the sense that we cannot expect convergence within a given precision, with a number of iterations bounded by a constant independent of  $M$ : for instance, the Gauss-Seidel iteration would need a number of iterations exactly proportional to  $M^\alpha$ . In addition, even the Krylov methods will suffer from the latter asymptotic ill-conditioning. In reality, looking at the estimates by Axelsson and Lindskög [23],  $O(M^{\alpha/2})$  iterations would be needed by a standard CG for reaching a solution within a fixed accuracy. In the present context of a zero of noninteger order, even the preconditioning by using band-Toeplitz matrices, will not ensure optimality as discussed in [7] and detailed in Section 4. On the other hand, when using circulant or the  $\tau$  preconditioning, the spectral equivalence is guaranteed also for a noninteger order of the zero at  $x = 0$  if the order is bounded by 2 [9, 10, 11]. In the latter case, the distance in rank is less with respect to other matrix-algebras as emphasized in [24]. In a multi-dimensional setting, only the  $\tau$  preconditioning leads to optimality using the PCG under the same constraint on the order of the zero, while

multilevel circulants are not well-suited [12]. Finally, since we consider also problems in imaging we recall that the  $\tau$  algebra emerges also in this context when using high precision boundary conditions (BCs) such as the anti-reflective BCs [25, 26].

### 3 Multigrid methods and level independency

Multigrid methods (MGMs) have already proven to be effective solvers as well as valid preconditioners for Krylov methods when numerically approaching FDEs [15, 8, 14]. A multigrid method combines two iterative methods called smoother and coarse grid correction. The two basic procedures when carefully chosen are spectrally complementary and in this sense, multigrid procedures are always of multi-iterative type [27]. The coarser matrices can either be obtained by projection (Galerkin approach) or by rediscrretization (geometric approach). In the case where only a single coarser level is considered we obtain Two Grids Methods (TGMs), while in the presence of more levels, we have multigrid methods, in particular, V-cycle when only a recursive call is performed and W-cycle when two recursive calls are applied.

Deepening what has been done in [7, 15], in this section, we investigate the convergence of multigrid methods in Galerkin form for the discretized problem (2.8).

To apply the Galerkin multigrid to a given linear system  $A_M x = b$ , for  $M_0 = M > M_1 > M_2 > \dots > M_\ell > 0$ , let us define the grid transfer operators  $P_k \in \mathbb{R}^{M_{k+1} \times M_k}$  as

$$P_k = K_k T_{M_k}(p_k), \quad k = 0, \dots, \ell - 1, \quad (3.1)$$

where  $K_k$  is the down-sampling operator and  $p_k$  is a properly chosen polynomial. The coarser matrices are then

$$A_{M_{k+1}} = P_k A_{M_k} P_k^T, \quad k = 0, \dots, \ell - 1. \quad (3.2)$$

If at the recursive level  $k$ , we simply apply one post-smoothing iteration of a stationary method having iteration matrix  $S_k$  the TGM iteration matrix at the level  $k$  is given by

$$TGM_k = S_k [I_{M_k} - P_k^T (P_k A_{M_k} P_k^T)^{-1} P_k A_{M_k}].$$

The following theorem states the convergence of TGM at a generic recursion level  $k$ .

**Theorem 3.1** (Ruge-Stüben [28]). *Let  $A_{M_k}$  be a symmetric positive definite matrix,  $D_k$  the diagonal matrix having as main diagonal that of  $A_{M_k}$ , and  $S_k$  be the post-smoothing iteration matrix. Assume that  $\exists \sigma_k > 0$  such that*

$$\|S_k u\|_{A_{M_k}}^2 \leq \|u\|_{A_{M_k}}^2 - \sigma_k \|u\|_{A_{M_k} D_k^{-1} A_{M_k}}^2, \quad \forall u \in \mathbb{R}^{M_k}, \quad (3.3)$$

and  $\exists \delta_k > 0$  such that

$$\min_{y \in \mathbb{R}^{M_{k+1}}} \|u - P_k y\|_{D_k}^2 \leq \delta_k \|u\|_{A_{M_k}}^2, \quad \forall u \in \mathbb{R}^{M_k}, \quad (3.4)$$

then  $\delta_k > \sigma_k$  and

$$\|TGM_k\|_{A_{M_k}} \leq \sqrt{1 - \frac{\sigma_k}{\delta_k}}.$$

The inequalities in equations (3.3) and (3.4) are well known as the smoothing property and approximation property, respectively. To prove the multigrid convergence (recursive application of TGM) it is enough to prove that the assumptions of Theorem 3.1 are satisfied for each  $k = 0, 1, \dots, \ell - 1$ . On the other hand, to guarantee a W-cycle convergence in a number of iterations independent of the size  $M$  [29], we have to prove that the following level independency condition

$$\liminf_{k \rightarrow \infty} \frac{\sigma_k}{\delta_k} = \beta > 0 \quad (3.5)$$

holds with  $\beta$  independent of  $k$ .

Concerning (multilevel) Toeplitz matrices, multigrid methods have been extensively investigated in the literature [30, 31, 32]. While the smoothing property can be easily carried on for a simple smoother like weighted Jacobi, the approximation property usually requires a detailed analysis based on a generalization of the local Fourier analysis, see [33].

If we now apply the multigrid with Galerkin approach to the solution of (2.8) and refer to the matrices at the coarser level  $k$  as  $A_{M_k}^\alpha$ , they are still Toeplitz and, based on the theoretical analysis developed in [34, 35] for  $\tau$  matrices, are associated to the following symbols

$$f_{k+1,\alpha}(x) = \frac{1}{2} \left[ f_{k,\alpha} \left( \frac{x}{2} \right) p_{k,\alpha}^2 \left( \frac{x}{2} \right) + f_{k,\alpha} \left( \pi - \frac{x}{2} \right) p_{k,\alpha}^2 \left( \pi - \frac{x}{2} \right) \right], \quad k = 0, \dots, \ell - 1. \quad (3.6)$$

Since the function  $f_{0,\alpha} = f_\alpha$  has only a zero at the origin of order smaller or equal to 2, according to the convergence analysis of multigrid methods in [34, 35], we define the symbols of the projectors  $P_k$  in (3.1) as

$$p_k(x) = p_{k,\alpha}(x), \quad \text{where} \quad p_{k,\alpha}(x) = C_{k+1,\alpha} p(x) = C_{k+1,\alpha} (1 + \cos x) \quad (3.7)$$

and  $C_{k+1,\alpha}$  is a constant chosen such that  $f_{k+1,\alpha}(\pi) = f_{k,\alpha}(\pi)$ .

We observe that the symbols  $f_{k,\alpha}$  at each level are nonnegative and they vanish only at the origin with order  $\alpha$  thanks to [36, Proposition 2.3]. Therefore, the symbols  $p_{k,\alpha}$  in (3.7) and  $f_{k+1,\alpha}$  in (3.6) satisfy the approximation property (3.4) because

$$\lim_{x \rightarrow 0} \frac{p_{k,\alpha}(x + \pi)^2}{f_{k+1,\alpha}(x)} = \gamma_k < \infty \quad (3.8)$$

at each level  $k = 0, \dots, \ell - 1$ , see [36, Proposition 3.1].

*Remark 1.* Since  $\delta_k$  is proportional to  $\gamma_k$ , the level independency condition (3.5) requires that

$$\limsup_{k \rightarrow \infty} \gamma_k = \gamma < \infty \quad (3.9)$$

with  $\gamma$  independent of  $k$ .

For the smoothing property (3.3), in order to ensure  $\sigma_k > \sigma > 0$  for all  $k$ , will be crucial the choice of  $C_{k+1,\alpha}$  as a constant such that  $f_{k+1,\alpha}(\pi) = f_{k,\alpha}(\pi)$ .

In conclusion, to prove the level independency condition (3.5), we need a detailed analysis of the symbol  $f_{k+1,\alpha}$ , which is performed in the next subsection.

### 3.1 Behaviour of symbols $f_{k,\alpha}$

The analysis of  $f_{k+1,\alpha}$  in (3.6) requires a detailed study of the constant  $C_{k+1,\alpha}$  in  $p_{k,\alpha}$  chosen imposing the condition

$$f_{k+1,\alpha}(\pi) = f_{k,\alpha}(\pi) = c(\alpha) 2^{\alpha+1}, \quad k = 0, 1, \dots, \ell - 1,$$

because  $f_{0,\alpha}(\pi) = c(\alpha) 2^{\alpha+1}$ .

According to the classical analysis, in the case of discrete Laplacian, i.e.,  $l(x) = 2 - 2 \cos x$ , the value of  $C_{k+1,2}$  at each level is  $\sqrt{2}$ .

**Proposition 3.2.** *Let  $f_{0,2}(x) = l(x)$ , where  $l(x) = 2 - 2 \cos x$ , and  $p_{k,2}(x) = C_{k+1,2} p(x)$  with  $C_{k+1,2} = \sqrt{2}$ . Then, for  $f_{k+1,2}$  computed according to (3.6), it holds*

$$f_{k+1,2}(x) = l(x), \quad k = 0, 1, \dots, \ell - 1. \quad (3.10)$$

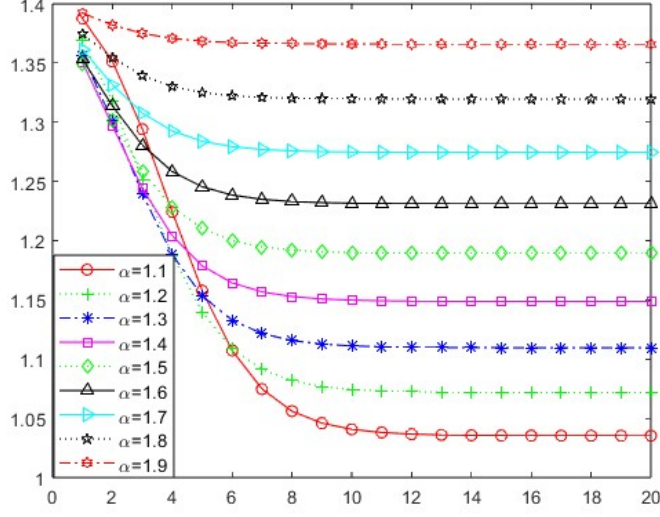


Figure 1: Plot of  $C_{k,\alpha}$  vs the level  $k$ , for different values of  $\alpha$ .

*Proof.* Since  $p_{k,2}(x) = \sqrt{2}p(x) = \sqrt{2}(1 + \cos x)$ , using relation (3.6), for  $k = 0$  it holds

$$f_{1,2}(x) = l\left(\frac{x}{2}\right)p^2\left(\frac{x}{2}\right) + l\left(\pi - \frac{x}{2}\right)p^2\left(\pi - \frac{x}{2}\right) = l(x).$$

Since the symbol  $p_{k,2}$  of the projector is the same at each level, by recursive relation we obtain the required result

$$f_{\ell,2}(x) = \dots = f_{1,2}(x) = f_{0,2}(x) = l(x).$$

□

For  $\alpha \in (1, 2]$ , the value of  $C_{k+1,\alpha}$ , computed such that  $f_{k+1,\alpha}(\pi) = f_{k,\alpha}(\pi)$ , is

$$C_{k+1,\alpha}^2 = \frac{f_{k+1,\alpha}(\pi)}{L_{k+1,\alpha}(\pi)} = \frac{2^{\alpha+1}}{L_{k+1,\alpha}(\pi)}, \quad k = 0, 1, 2, \dots, \ell - 1, \quad (3.11)$$

where

$$L_{k+1,\alpha}(x) = \frac{1}{2} \left[ f_{k,\alpha}\left(\frac{x}{2}\right)p^2\left(\frac{x}{2}\right) + f_{k,\alpha}\left(\pi - \frac{x}{2}\right)p^2\left(\pi - \frac{x}{2}\right) \right].$$

Since  $L_{k+1,\alpha}(\pi) = f_{k,\alpha}\left(\frac{\pi}{2}\right)$  converges to 4 as  $k$  diverges, then we have

$$\lim_{k \rightarrow \infty} C_{k,\alpha} = 2^{\frac{\alpha-1}{2}}, \quad \text{for } \alpha \in (1, 2], \quad (3.12)$$

as can be seen in Figure 1. Moreover, the convergence of  $C_{k,\alpha}$  is quite fast, especially for  $\alpha$  close to 2.

We observe that the sequence of the coarser symbols satisfies

$$\frac{f_{\ell,\alpha}(x)}{c(\alpha)} \geq \frac{f_{\ell-1,\alpha}(x)}{c(\alpha)} \geq \dots \geq \frac{f_{0,\alpha}(x)}{c(\alpha)} \geq l(x),$$



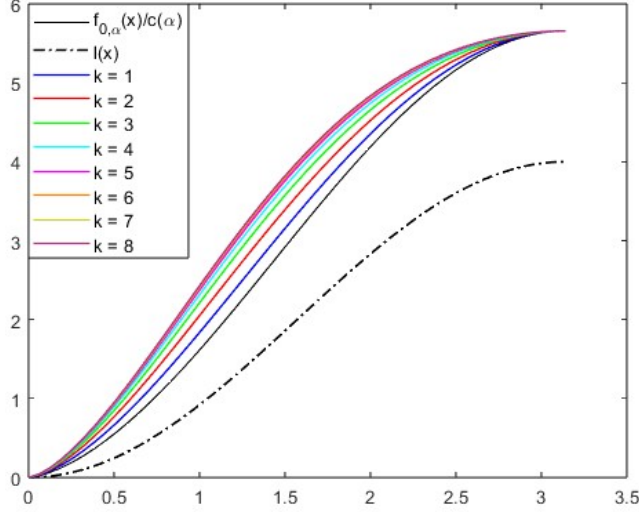


Figure 2: Plots of  $f_{k+1,\alpha}/c(\alpha)$  for  $\alpha = 1.5$  and  $k = 0, \dots, 8$ , with  $C_{k,\alpha}$  computed according to (3.11).

for any  $\alpha \in (1, 2)$ , as can be seen in Figure 2. Combining this fact with

$$\|f_{k,\alpha}\|_{\infty} = f_{k,\alpha}(\pi) = f_{0,\alpha}(\pi) = c(\alpha)2^{\alpha+1}, \quad k = 1 \dots, \ell$$

for any  $\alpha \in (1, 2)$ , we obtain that the ill-conditioning of the coarser linear systems decreases moving on coarser grids.

### 3.2 Smoothing Property

If weighted Jacobi is used as smoother, then the smoothing property (3.3) is satisfied whenever the smoother converges [31, 28]. Since the matrix  $A_{M_k}^{\alpha}$  is symmetric positive definite, the weighted Jacobi method

$$S_k = I_{M_k} - \omega_k D_k^{-1} A_{M_k}^{\alpha}$$

is well-defined, with  $D_k$  being the diagonal of  $A_{M_k}^{\alpha}$ . Moreover, it converges for  $0 < \omega_k < 2/\rho(D_k^{-1} A_{M_k}^{\alpha})$ , where  $\rho(D_k^{-1} A_{M_k}^{\alpha})$  is the spectral radius of  $D_k^{-1} A_{M_k}^{\alpha}$ .

When  $A_{M_k}^{\alpha} = T_{M_k}(f_{0,\alpha})$ , as for the geometric approach, then  $D_k = a_0^{(0)} I_{M_k}$ , where  $a_0^{(0)}$  is the Fourier coefficient of order zero of  $f_{0,\alpha}$ , and thus it holds

$$S_k = I_{M_k} - \frac{\omega_k}{2\alpha} A_{M_k}^{\alpha}, \quad (3.13)$$

since  $a_0^{(0)} = 2c(\alpha)\alpha$ .

**Lemma 3.3.** *Let  $A_{M_k}^{\alpha} = T_{M_k}(f_{0,\alpha})$  with  $f_{0,\alpha} = f_{\alpha}$  defined as in (2.14) and let  $S_{M_k}$  defined as in (3.13). If we choose*

$$0 < \omega_k < \frac{\alpha}{2^{\alpha-1}}, \quad (3.14)$$

*then there exist  $\sigma_k$  such that the smoothing property in (3.3) holds true.*

Moreover, choosing

$$\omega_k = \frac{2^{2-\alpha}\alpha}{3}, \quad (3.15)$$

it holds

$$\sigma_k \geq \sigma = \frac{2^{-\alpha}}{9} > 0. \quad (3.16)$$

*Proof.* Since  $f_{0,\alpha}$  is nonnegative, from Lemma 4.2 in [15] it follows

$$0 < \omega_k < \frac{2a_0^{(0)}}{\|f_{0,\alpha}\|_\infty} = \frac{\alpha}{2^{\alpha-1}},$$

since  $\|f_{0,\alpha}\|_\infty = f_{0,\alpha}(\pi) = c(\alpha)2^{\alpha+1}$ . Moreover, for  $\omega_k$  chosen as in (3.15), the following condition

$$\left(I_{M_k} - \frac{\omega_k}{2\alpha} A_{M_k}^\alpha\right)^2 \leq I_{M_k} - \frac{\sigma_k}{2\alpha} A_{M_k}^\alpha$$

in the proof of Lemma 4.2 in [15] is satisfied for all  $\sigma_k \geq \sigma$  in (3.16).  $\square$

From the previous lemma, following the same idea as given in [37], we propose to use the following Jacobi parameter

$$\omega_k = \omega^* = \frac{2^{2-\alpha}\alpha}{3}, \quad \forall k \geq 0, \quad (3.17)$$

which provides a good convergence rate as confirmed in the numerical results in Section 5.

### 3.3 Approximation property and level independency

According to Remark 1, the uniform boundness of  $\delta_k$  is ensured by proving equation (3.9).

First of all, we prove that for  $k \in \mathbb{N}_0$ , the sequence of functions  $g_{k,\alpha}(x) = \frac{p_{k,\alpha}^2(\pi-x)}{f_{k,\alpha}(x)}$  is monotonic increasing in  $x$ . Recalling the expression of  $p_{k,\alpha}$  in (3.7), differentiating  $g_{k,\alpha}$  we have

$$\frac{d}{dx} g_{k,\alpha}(x) = \frac{C_{k+1,\alpha}^2(1-\cos x)}{f_{k,\alpha}^2(x)} (2 \sin x f_{k,\alpha}(x) - (1-\cos x) \frac{d}{dx} f_{k,\alpha}(x)),$$

and hence it is equivalent to proving that

$$\mathbf{g}_{k,\alpha}(x) = 2 \sin x f_{k,\alpha}(x) - (1-\cos x) \frac{d}{dx} f_{k,\alpha}(x)$$

is nonnegative for all  $k \in \mathbb{N}_0$ . This result can be proved by induction on  $k$ .

For  $k = 0$ , replacing the expression of  $f_{0,\alpha}$  (see equation (2.14)) in  $\mathbf{g}_{k,\alpha}$ , by direct computations we obtain  $\mathbf{g}_{k,\alpha}(x) \geq 0, \forall x \in [0, \pi]$ .

Assuming that for  $k = n$  it holds  $\mathbf{g}_{n,\alpha}(x) \geq 0, \forall x \in [0, \pi]$ , we have to prove that the same is true for  $k = n + 1$ .

Applying the recurrence (3.6) to  $f_{n+1,\alpha}$ , we have

$$\mathbf{g}_{n+1,\alpha}(x) \geq p^2 \left(\frac{x}{2}\right) S_1(x) - p^2 \left(\pi - \frac{x}{2}\right) S_2(x),$$

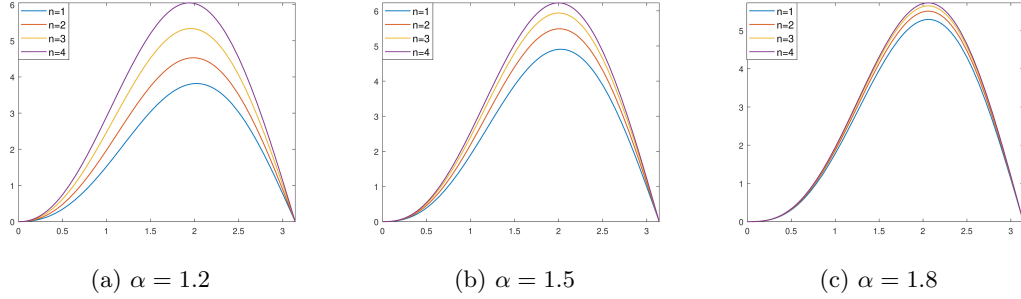


Figure 3: Plot of  $\mathbf{g}_{n,\alpha}(x)$  for different values of  $\alpha$ .

where  $p(x) = 1 + \cos(x)$ , as defined in (3.7), and

$$S_1(x) = \sin\left(\frac{x}{2}\right) f_{n,\alpha}\left(\frac{x}{2}\right) - \frac{1}{2}\left(1 - \cos\left(\frac{x}{2}\right)\right) \frac{d}{dx} f_{n,\alpha}\left(\frac{x}{2}\right),$$

$$S_2(x) = \sin\left(\frac{x}{2}\right) f_{n,\alpha}\left(\pi - \frac{x}{2}\right) + \frac{1}{2}\left(1 + \cos\left(\frac{x}{2}\right)\right) \frac{d}{dx} f_{n,\alpha}\left(\pi - \frac{x}{2}\right).$$

Thanks to the inductive assumption and direct computation, we obtain the desired result  $\mathbf{g}_{n+1,\alpha}(x) \geq 0$ ,  $\forall x \in [0, \pi]$ , i.e.,

$$\frac{d}{dx} g_{k,\alpha}(x) \geq 0, \quad \forall k \in \mathbb{N}_0.$$

Figure 3 depicts the function  $\mathbf{g}_{k,\alpha}$  for different values of  $k$  and  $\alpha$ .

In conclusion, by the monotonicity of  $g_{k,\alpha}(x)$ , for all  $k \geq 0$ , we have

$$\max_{x \in [0, \pi]} g_{k,\alpha}(x) = g_{k,\alpha}(\pi) = \frac{p_{k,\alpha}^2(0)}{f_{k,\alpha}(\pi)} = \frac{4C_{k,\alpha}^2}{c(\alpha)2^{\alpha+1}},$$

and since the sequence  $C_{k,\alpha}$  is bounded thanks to equation (3.12) (see also Figure 1), we have that  $\{\gamma_k\}_k$ , and hence  $\{\delta_k\}_k$ , is bounded.

Combining the previous result on  $\delta_k$  with equation (3.16) for the smoothing analysis, it holds (3.5), i.e., the level independency is satisfied.

## 4 Band Approximation

Multigrid methods are often applied as preconditioners for Krylov methods, and often to an approximation of  $A_M^\alpha$  instead of at the original coefficient matrix. On the same line as what has been done in [8], in this section, we discuss a band approximation of  $A_M^\alpha$  to combine with the multigrid method discussed in the previous section. The advantage of using a band matrix is in the possibility of applying the Galerkin approach with a linear cost in  $M$  instead of  $O(M \log M)$  and inheriting the V-cycle optimality from the results in [35].

Starting from the truncated Fourier sum of order  $s$  of the symbol  $f_\alpha$

$$g_s(x) = 2 \sum_{k=0}^s g_k^{(\alpha)} \cos((k-1)x), \quad (4.1)$$

we consider as band approximation of  $A_M^\alpha$  the associated Toeplitz matrix  ${}_s\mathbf{B}_M^\alpha = T_M(g_s)$  explicitly given by

$${}_s\mathbf{B}_M^\alpha = - \left[ \begin{array}{ccccccc} 2g_1^{(\alpha)} & g_0^{(\alpha)} + g_2^{(\alpha)} & \cdots & g_s^{(\alpha)} & & & \\ g_0^{(\alpha)} + g_2^{(\alpha)} & 2g_1^{(\alpha)} & g_0^{(\alpha)} + g_2^{(\alpha)} & \cdots & g_s^{(\alpha)} & & \\ \vdots & \ddots & \ddots & \ddots & \ddots & & g_s^{(\alpha)} \\ g_s^{(\alpha)} & \ddots & \ddots & \ddots & \ddots & & \vdots \\ & g_s^{(\alpha)} & \ddots & g_0^{(\alpha)} + g_2^{(\alpha)} & 2g_1^{(\alpha)} & g_0^{(\alpha)} + g_2^{(\alpha)} & \\ & & g_s^{(\alpha)} & \cdots & g_0^{(\alpha)} + g_2^{(\alpha)} & 2g_1^{(\alpha)} & \end{array} \right]_{M \times M}. \quad (4.2)$$

The emerging banded matrix is defined as

$${}_s\tilde{A}_M^\alpha = \bar{c} {}_s\mathbf{B}_M^\alpha, \quad (4.3)$$

As already discussed in [15, 8], concerning the application of our multigrid method to a linear system with the coefficient matrix  ${}_s\tilde{A}_M^\alpha$ , we have the following feature thanks to the results in [35, 32]:

- The computation of the coarser matrices by the Galerkin approach (3.2), using the projector defined in (3.1), preserves the band structure at the coarser levels, see [32, Proposition 2].
- If the function  $g_s$  is nonnegative, then the V-cycle is optimal, i.e., has a constant convergence rate independent of the size  $M$  and a computational cost per iteration proportional to  $O(sM)$ , that is  $O(M \log M)$  with the choice of  $s$  such that  $M = 2^s - 1$ .

About the spectral features of preconditioned Toeplitz matrices with Toeplitz preconditioners, we recall the well-known results of both localization and distribution type in the sense of Weyl in the following theorem (see [38, 5]).

**Theorem 4.1.** *Let  $f$  be real-valued,  $2\pi$ -periodic, and continuous and  $g$  be nonnegative,  $2\pi$ -periodic, continuous, with  $\max g > 0$ . Then*

- $T_M(g)$  is positive definite for every  $M$ ;
- if  $r = \inf \frac{f}{g}$ ,  $R = \sup \frac{f}{g}$  with  $r < R$ , then all the eigenvalues of  $T_M^{-1}(g)T_M(f)$  lie in the open set  $(r, R)$  for every  $M$ ;
- $\{T_M(f)\}_M, \{T_M(g)\}_M, \{T_M^{-1}(g)T_M(f)\}_M$  are distributed in the Weyl sense as  $f, g, \frac{f}{g}$ , respectively, i.e. for all  $F$  in the set of continuous functions with compact support over  $\mathbb{C}$  it holds

$$\lim_{n \rightarrow \infty} \frac{1}{M} \sum_{j=1}^M F(\lambda_j(\mathcal{A}_M)) = \frac{1}{b-a} \int_a^b F(\kappa(t)) dt. \quad (4.4)$$

with  $A_M = T_M(f), T_M(g), T_M^{-1}(g)T_M(f)$ ,  $\kappa = f, g, \frac{f}{g}$ ,  $\lambda_j(\mathcal{A}_M)$  the eigenvalues of  $A_M$ , and  $[a, b] = [-\pi, \pi]$ .

In other words, a good Toeplitz preconditioner for a Toeplitz matrix generated by  $f$  should be generated by  $g$  such that  $\frac{f}{g}$  is close to 1 in a certain metric, for instance in  $L^\infty$  or in  $L^1$  norm.

About the band preconditioner in (4.2), Figure 4 shows the graphs of  $g = g_s$  and  $f = f_\alpha$  for two different values of  $\alpha$ , while  $\delta_s = f_\alpha - g_s$  are depicted in Figure 5, for some values of  $s$ . Obviously, the quality of the approximation grows increasing  $s$ , but it is good enough already for a small  $s$ , in particular when  $\alpha$  approaches the value 2 (see the scale of the  $y$ -axis in Figure 5).

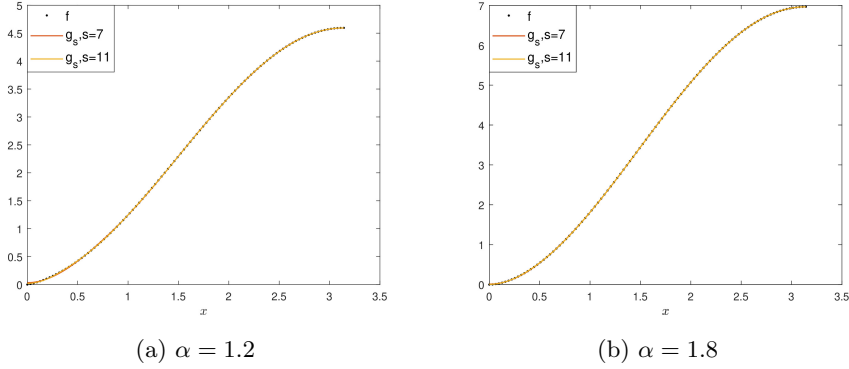


Figure 4: Plots of  $f$  and  $g_s$ .

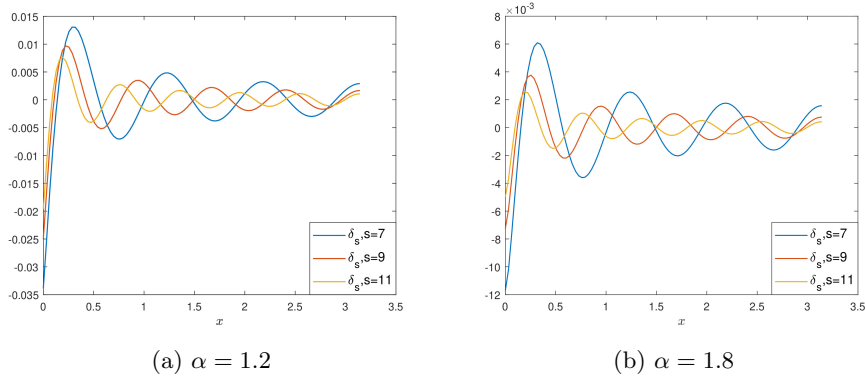


Figure 5: Plots of  $\delta_s$ .

More importantly, in the light of Theorem 4.1, Figure 6 depicts the functions  $\kappa_s - 1$  with  $\kappa_s = \frac{f_\alpha}{g_s}$ . This quantity measures the relative approximation, which is the one determining the quality of the preconditioning since  $(\kappa_s - 1, [0, \pi])$  is the distribution function of the shifted preconditioned matrix-sequence

$$\{T_M^{-1}(g)T_M(f) - I_M\}_M, \quad g = g_s, \quad f = f_\alpha,$$

in the sense of Weyl and in accordance again with Theorem 4.1. Note that the function  $\kappa_s - 1$  is almost zero except around the zero of  $f_\alpha$  at the origin.

## 5 Numerical Examples

In this section, we present some numerical examples, to verify the effectiveness of the MGM used both as a solver and preconditioner. In what follows:

- $V_{\nu_1}^{\nu_2}$  consists of a Galerkin V-cycle with linear interpolation as grid transfer operator and  $\nu_1$  and  $\nu_2$  iterations of pre and post-smoother weighted Jacobi, respectively;
- $P_C$  and  $P_S$  represent the Chan [39] and Strang circulant preconditioner, respectively;
- $P_s V_{\nu_1}^{\nu_2}$  denotes the banded preconditioner defined as in equation (4.2) and inverted using MGM with Galerkin approach  $V_{\nu_1}^{\nu_2}$ ;

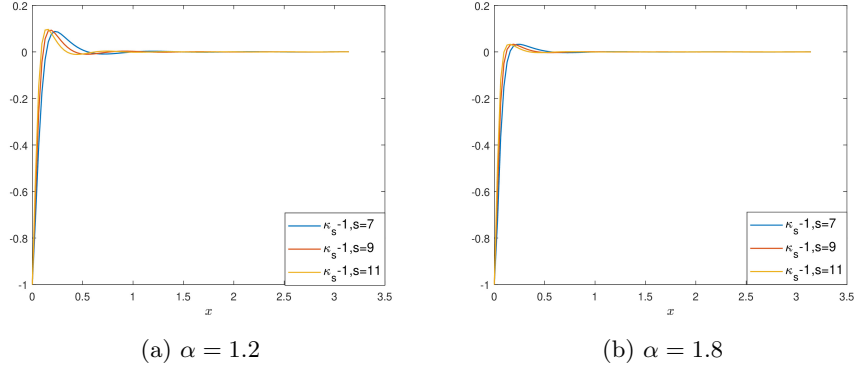


Figure 6: Plots of  $\kappa_s - 1$ .

- $PV_{\nu_1}^{\nu_2}$  and  $\tilde{P}V_{\nu_1}^{\nu_2}$  are multigrid preconditioners, both as Galerkin and Geometric approach, respectively.

The aforementioned preconditioners are combined with CG and GMRES computationally performed using built-in *pcg* and *gmres* Matlab functions. The stopping criterion is chosen as

$$\frac{\|r^k\|}{\|r^0\|} < 10^{-8},$$

where  $\|\cdot\|$  denotes the Euclidean norm,  $r^k$  is the residual vector at the  $k$ -th iteration. The initial guess is fixed as the zero vector. All the numerical experiments are run by using MATLAB R2021a on HP 17-cp0000nl computer with configuration, AMD Ryzen 7 5700U with Radeon Graphics CPU and 16GB RAM.

**Example 1.** Consider the following 1D-RFDE given in equation (2.1), with  $\Omega = [0, 1]$  and the source term built from the exact solution

$$u(x) = x^2(1 - x)^2. \quad (5.1)$$

Table 1 shows the number of iterations of the proposed multigrid methods and preconditioners for three different values of  $\alpha$ .

Regarding multigrid methods, the observations are as follows:

- The Galerkin approach is robust, even as V-cycle, in agreement with the previous theoretical analysis.
- The geometric approach is robust only when  $\alpha > 1.5$ .
- The robustness of the geometric multigrid can be improved by using it as a preconditioner, as seen in the column  $\tilde{P}V_1^1$ . In particular, it is even more robust than the band multigrid preconditioner  $P_s V_1^1$ .

When comparing the circulant preconditioners, the Strang preconditioner  $P_S$  is preferable to the optimal Chan preconditioner  $P_C$ .

## 5.1 2D Problems

Here we extend our study to two-dimensional variable coefficient RFDE, given by

$$-c(x, y) \frac{\partial^\alpha u(x, y)}{\partial |x|^\alpha} - e(x, y) \frac{\partial^\beta u(x, y)}{\partial |y|^\beta} = m(x, y), \quad (x, y) \in \Omega = [a_1, b_1] \times [a_2, b_2], \quad (5.2)$$

Table 1: Example 1: Number of iterations for  $\alpha = 1.2, 1.5,$  and  $1.8$  with  $\omega^* = 0.6964, 0.7071,$  and  $0.6892,$  respectively.

$\alpha$	$M + 1$	Galerkin						Geometric						Preconditioners									
		CG	TGM			V-Cycle			$V_0^1$	$V_1^0$	$V_1^1$	TGM			V-Cycle			$s$	$P_s V_1^1$	$PV_1^1$	$\tilde{P}V_1^1$	$P_C$	$P_S$
			$V_0^1$	$V_1^0$	$V_1^1$	$V_0^1$	$V_1^0$	$V_1^1$				$V_0^1$	$V_1^0$	$V_1^1$									
$\alpha = 1.2$	$2^6$	32	17	17	9	17	17	9	16	16	13	37	38	31	7	8	6	11	9	5			
	$2^7$	63	16	16	9	16	17	10	16	16	13	43	43	34	7	8	6	12	10	6			
	$2^8$	110	16	16	9	16	17	10	16	16	12	48	48	37	9	10	6	12	12	6			
	$2^9$	178	16	16	9	16	18	10	16	16	12	52	52	40	9	13	7	12	13	6			
	$2^{10}$	279	15	15	8	16	18	11	15	15	11	55	56	42	11	18	7	12	14	7			
$\alpha = 1.5$	$2^6$	32	17	17	9	17	17	10	17	17	10	23	22	16	7	7	6	8	9	5			
	$2^7$	62	17	17	9	16	17	9	17	17	10	25	24	17	7	8	6	8	11	5			
	$2^8$	111	17	17	9	16	17	10	17	17	10	27	26	19	9	10	6	8	13	7			
	$2^9$	192	16	16	9	16	18	10	16	16	9	28	28	20	9	14	6	9	14	7			
	$2^{10}$	328	16	16	9	16	18	10	16	16	9	30	30	20	11	19	7	9	16	8			
$\alpha = 1.8$	$2^6$	32	17	17	10	17	17	11	17	17	10	18	21	13	7	8	7	7	10	6			
	$2^7$	64	17	17	10	17	18	11	17	17	10	19	20	13	7	9	7	8	13	6			
	$2^8$	126	17	17	10	17	18	11	17	17	10	20	22	13	9	10	7	8	15	7			
	$2^9$	238	17	17	9	17	19	11	17	17	9	21	23	14	9	14	7	8	17	7			
	$2^{10}$	448	17	17	9	18	20	12	17	17	9	22	24	14	11	18	7	8	21	7			

with boundary condition

$$u(x, y) = 0, \quad (x, y) \in \partial\Omega, \quad (5.3)$$

where  $c(x, y), e(x, y)$  are non-negative diffusion coefficients,  $m(x, y)$  is the source term, and  $\frac{\partial^\gamma u(x, y)}{\partial |x|^\gamma}, \frac{\partial^\gamma u(x, y)}{\partial |y|^\gamma}$  are the Riesz fractional derivatives for  $\gamma \in \{\alpha, \beta\}, \alpha, \beta \in (1, 2)$ . In order to define the uniform partition of the spatial domain  $\Omega$ , we fix  $M_1, M_2 \in \mathbb{N}$  and define

$$\begin{aligned} x_j &= a_1 + jh_x, & h_x &= \frac{b_1 - a_1}{M_1 + 1}, & j &= 0, \dots, M_1 + 1, \\ y_j &= a_2 + jh_y, & h_y &= \frac{b_2 - a_2}{M_2 + 1}, & j &= 0, \dots, M_2 + 1. \end{aligned}$$

Let us now introduce the following  $M$ -dimensional vectors, with  $M = M_1 M_2$ :

$$\begin{aligned} \mathbf{u} &= [u_{1,1}, u_{2,1}, \dots, u_{M_1,1}, u_{1,2}, u_{2,2}, \dots, u_{M_1,2}, \dots, u_{1,M_2}, u_{2,M_2}, \dots, u_{M_1,M_2}]^T, \\ \mathbf{c} &= [c_{1,1}, c_{2,1}, \dots, c_{M_1,1}, c_{1,2}, c_{2,2}, \dots, c_{M_1,2}, \dots, c_{1,M_2}, c_{2,M_2}, \dots, c_{M_1,M_2}]^T, \\ \mathbf{e} &= [e_{1,1}, e_{2,1}, \dots, e_{M_1,1}, e_{1,2}, e_{2,2}, \dots, e_{M_1,2}, \dots, e_{1,M_2}, e_{2,M_2}, \dots, e_{M_1,M_2}]^T, \\ \mathbf{m} &= [m_{1,1}, m_{2,1}, \dots, m_{M_1,1}, m_{1,2}, m_{2,2}, \dots, m_{M_1,2}, \dots, m_{1,M_2}, m_{2,M_2}, \dots, m_{M_1,M_2}]^T, \end{aligned}$$

where  $u_{i,j} = u(x_i, y_j)$ ,  $c_{i,j} = c(x_i, y_j)$ , and  $e_{i,j} = e(x_i, y_j)$ .

Using the shifted Grünwald difference formula for both fractional derivatives in  $x$  and  $y$  leads to the matrix-vector form

$$A_M^{(\alpha, \beta)} \mathbf{u} = \mathbf{m}, \quad (5.4)$$

with the following (diagonal times two-level Toeplitz structured) coefficient matrix

$$A_M^{(\alpha, \beta)} = \bar{c}_\alpha [C(I_{M_2} \otimes (\mathcal{G}_{M_1}^\alpha + (\mathcal{G}_{M_1}^\alpha)^T))] + \bar{c}_\beta [E((\mathcal{G}_{M_2}^\beta + (\mathcal{G}_{M_2}^\beta)^T) \otimes I_{M_1})], \quad (5.5)$$

where  $C = \text{diag}(\mathbf{c})$ ,  $E = \text{diag}(\mathbf{e})$ ,  $\bar{c}_\alpha = \frac{c(\alpha)}{h_x^\alpha}$ ,  $\bar{c}_\beta = \frac{c(\beta)}{h_y^\beta}$  and  $c(\gamma)$ ,  $\mathcal{G}_{M_i}^\gamma$  is defined as in Section 2.

Note that, the coefficient matrix  $A_M^{(\alpha,\beta)}$  is strictly diagonally dominant M-matrix. Moreover, when the diffusion coefficients are constant and equal, the coefficient matrix  $A_M^{(\alpha,\beta)}$  is a symmetric positive definite Block-Toeplitz with Toeplitz Blocks (BTB) matrix.

In the following examples, we compare the performance of the MGMs, banded, circulant, and  $\tau$ -based preconditioners. Precisely,

- Multigrid preconditioners,  $PV_1^1$  and  $P\tilde{V}_1^1$ . In both cases, the grid transfer operator is a bilinear interpolation, the weighted Jacobi is used as smoother, and one iteration of the V-cycle is performed to approximate the inverse of  $A_M^{(\alpha,\beta)}$ . Following the 1D case, the relaxation parameter of Jacobi  $\omega^*$  is computed as

$$\omega^* = \frac{4}{5}\zeta, \quad (5.6)$$

where  $\zeta = \frac{2\hat{\mathcal{F}}_0}{\|\mathcal{F}_{\alpha,\beta}(x,y)\|_\infty}$ , with  $\hat{\mathcal{F}}_0$  being the first Fourier coefficient of  $\mathcal{F}_{\alpha,\beta}(x,y)$ , the symbol of  $A_M^{(\alpha,\beta)}$  (see [15] for more details).

- According to the 1D numerical results, the Strang circulant preconditioner outperforms the optimal Chan preconditioner. Therefore, in the following, we consider only the 2-level Strang circulant preconditioner defined as

$$P_S = \bar{c}_\alpha c^{av} (I_{M_2} \otimes (S(\mathcal{G}_{M_1}^\alpha) + S(\mathcal{G}_{M_1}^\alpha)^T)) + \bar{c}_\beta e^{av} ((S(\mathcal{G}_{M_2}^\beta) + S(\mathcal{G}_{M_2}^\beta)^T) \otimes I_{M_1}), \quad (5.7)$$

where  $c^{av} = \text{mean}(\mathbf{c})$ ,  $e^{av} = \text{mean}(\mathbf{e})$ , and  $S(T_M)$  is the Strang circulant approximation of the Toeplitz matrix  $T_M$ .

- Like in the 1D case, here we extend the banded preconditioner  $P_s V_1^1$  strategy to the 2D case. To approximate the inverse of  ${}_s \tilde{A}_M^{(\alpha,\beta)}$ , we performed  $V_1^1$  iterations of V-cycle with Galerkin approach, weighted Jacobi as smoother and bilinear interpolation as grid transfer operator.

The 2D-banded matrix is defined as

$${}_s \tilde{A}_M^{(\alpha,\beta)} = \bar{c}_\alpha C (I_{M_2} \otimes ({}_s \mathcal{G}_{M_1}^\alpha + ({}_s \mathcal{G}_{M_1}^\alpha)^T)) + \bar{c}_\beta E (({}_s \mathcal{G}_{M_2}^\beta + ({}_s \mathcal{G}_{M_2}^\beta)^T) \otimes I_{M_1}),$$

- $P_\tau$  denotes the  $\tau$  based preconditioner. For the symmetric Toeplitz matrix  $\mathbf{G}_{M_i}^{(\gamma)} = {}_s \mathcal{G}_{M_i}^\gamma + ({}_s \mathcal{G}_{M_i}^\gamma)^T$ , with  $i = 1, 2$ , the  $\tau$  matrix is

$$\tau(\mathbf{G}_{M_i}^{(\gamma)}) = \mathbf{G}_{M_i}^{(\gamma)} - H_{M_i}, \quad (5.8)$$

where  $H_{M_i}$  is a Hankel matrix, whose entries along antidiagonals are constant and equal to

$$-[g_3^{(\gamma)}, g_4^{(\gamma)}, \dots, g_{M_i}^{(\gamma)}, 0, 0, 0, g_{M_i}^{(\gamma)}, \dots, g_4^{(\gamma)}, g_3^{(\gamma)}].$$

Thanks to [40], the  $\tau$  matrix can be diagonalized as follows

$$\tau(\mathbf{G}_{M_i}^{(\gamma)}) = S_{M_i} D_{M_i} S_{M_i}, \quad (5.9)$$

where  $D_{M_i} = \text{diag}(\lambda(\mathbf{G}_{M_i}^{(\gamma)} - H_{M_i}))$  and  $S_{M_i}$  is the sine transform matrix whose entries are

$$S_{M_i} = \left[ \sqrt{\frac{2}{M_i + 1}} \sin \left( \frac{ij\pi}{M_i + 1} \right) \right]_{i,j=1}^{M_i}. \quad (5.10)$$



Table 2: Example 2: Number of iterations for different values of  $\alpha$  and  $\beta$  with  $M_1 = M_2$ .

$(\alpha, \beta)$	$M_1 + 1$	Galerkin			Geometric		Preconditioners									
		CG	$V_1^1$	T(s)	$V_1^1$	T(s)	$PV_1^1$	T(s)	$\tilde{P}V_1^1$	T(s)	$P_s V_1^1$	T(s)	$P_\tau$	T(s)	$P_S$	T(s)
$(1.1, 1.2)$ $\omega^* = 0.83$	$2^5$	57	17	0.036	36	0.134	9	0.083	13	0.144	10	0.085	6	0.091	13	0.085
	$2^6$	93	14	0.126	43	0.322	9	0.167	14	0.229	11	0.121	7	0.100	17	0.114
	$2^7$	157	14	0.809	48	0.815	8	0.604	15	0.465	12	0.325	7	0.144	19	0.297
	$2^8$	237	14	5.201	52	3.085	8	3.701	16	1.587	17	1.451	8	0.424	21	0.604
	$2^9$	383	14	46.42	56	11.09	9	60.46	17	5.645	26	38.62	8	1.055	24	2.002
$(1.5, 1.5)$ $\omega^* = 0.85$	$2^5$	44	14	0.035	19	0.083	8	0.082	8	0.127	9	0.079	6	0.088	12	0.081
	$2^6$	78	14	0.121	21	0.194	8	0.151	9	0.178	10	0.119	6	0.102	13	0.111
	$2^7$	136	12	0.737	23	0.418	8	0.592	10	0.331	12	0.308	7	0.143	16	0.286
	$2^8$	234	13	4.843	25	1.625	8	3.313	10	1.025	15	1.424	8	0.416	20	0.610
	$2^9$	401	13	43.68	26	5.710	8	56.52	11	3.811	25	34.69	8	1.071	25	2.057
$(1.7, 1.9)$ $\omega^* = 0.83$	$2^5$	66	24	0.041	26	0.114	11	0.089	11	0.139	11	0.085	6	0.091	15	0.089
	$2^6$	127	27	0.205	30	0.235	12	0.181	12	0.215	13	0.128	6	0.104	19	0.118
	$2^7$	244	30	1.557	34	0.598	13	0.904	13	0.407	15	0.385	6	0.140	25	0.383
	$2^8$	467	33	11.62	38	2.350	14	5.616	15	1.405	17	1.503	7	0.401	30	0.684
	$2^9$	899	37	124.3	43	8.658	15	87.13	16	5.464	27	40.18	7	1.103	43	3.594

The  $\tau$  based preconditioner of the resulting linear system (5.4) is

$$P_\tau = \mathcal{D}_M \mathbf{S}_M \mathbf{D}_M \mathbf{S}_M, \quad (5.11)$$

with  $\mathbf{S}_M = S_{M_1} \otimes S_{M_2}$ ,  $\mathbf{D}_M = (I_{M_2} \otimes D_{M_1} + D_{M_2} \otimes I_{M_1})$  and  $\mathcal{D}_M$  is the diagonal matrix that contains the average of the diffusion coefficients. Regarding the computational point of view,  $P_\tau$  is extremely suitable because the matrix-vector product can be performed in  $O(M \log M)$  operations through the discrete sine transform (DST) algorithm.

**Example 2.** In this example, we consider the following 2D-RFDE given in equation (5.2), with  $c(x, y) = e(x, y) = 1$  and  $\Omega = [0, 1] \times [0, 1]$ . The source term and exact solution are given as

$$u(x, y) = x^2(1-x)^2y^2(1-y)^2, \quad (5.12)$$

and

$$\begin{aligned} m(x, y) = & \frac{1}{\cos(\frac{\alpha\pi}{2})} y^2(1-y)^2 \left[ \frac{2}{\Gamma(3-\alpha)} \left( x^{2-\alpha} + (1-x)^{2-\alpha} \right) - \frac{12}{\Gamma(4-\alpha)} \left( x^{3-\alpha} + (1-x)^{3-\alpha} \right) \right. \\ & \left. + \frac{24}{\Gamma(5-\alpha)} \left( x^{4-\alpha} + (1-x)^{4-\alpha} \right) \right] + \frac{1}{\cos(\frac{\beta\pi}{2})} x^2(1-x)^2 \left[ \frac{2}{\Gamma(3-\beta)} \left( y^{2-\beta} + (1-y)^{2-\beta} \right) \right. \\ & \left. - \frac{12}{\Gamma(4-\beta)} \left( y^{3-\beta} + (1-y)^{3-\beta} \right) + \frac{24}{\Gamma(5-\beta)} \left( y^{4-\beta} + (1-y)^{4-\beta} \right) \right]. \end{aligned}$$

Table 2 presents the number of iterations and CPU times required by the proposed multigrid methods and preconditioners. The  $\tau$  preconditioner  $P_\tau$  stands out as the most robust choice, both in terms of iteration number and CPU time. The geometric multigrid used as a preconditioner is also a good option, although the robustness of multigrid methods declines in the case of anisotropic problems, i.e., when  $(\alpha, \beta) = (1.7, 1.9)$ . In such a case, it is advisable to adopt the strategies proposed in [8].

Table 3: Example 3: Number of iterations for different values of  $\alpha$  and  $\beta$  with  $M_1 = M_2$ .

$(\alpha, \beta)$	$M_1 + 1$	GMRES	$\tilde{P}V_1^1$	T(s)	$P_s V_1^1$	T(s)	$P_\tau$	T(s)	$P_S$	T(s)
$(1.1, 1.2)$ $\omega^* = 0.83$	$2^4$	49	11	0.147	9	0.100	12	0.114	19	0.118
	$2^5$	94	12	0.181	11	0.110	13	0.135	23	0.140
	$2^6$	163	14	0.258	12	0.159	13	0.160	27	0.201
	$2^7$	267	15	0.537	15	0.407	13	0.250	31	0.441
$(1.5, 1.5)$ $\omega^* = 0.85$	$2^4$	51	11	0.147	10	0.101	13	0.118	20	0.120
	$2^5$	95	12	0.182	12	0.112	13	0.133	24	0.146
	$2^6$	171	12	0.240	13	0.164	14	0.168	27	0.196
	$2^7$	301	12	0.531	17	0.412	14	0.261	31	0.423
$(1.7, 1.9)$ $\omega^* = 0.83$	$2^4$	62	13	0.146	12	0.103	12	0.116	21	0.122
	$2^5$	129	14	0.189	14	0.115	13	0.134	26	0.150
	$2^6$	262	15	0.281	14	0.164	14	0.167	31	0.214
	$2^7$	524	15	0.544	18	0.425	14	0.253	37	0.483
$(1.9, 1.9)$ $\omega^* = 0.82$	$2^4$	60	11	0.144	11	0.103	12	0.144	21	0.121
	$2^5$	124	12	0.183	11	0.109	13	0.132	25	0.148
	$2^6$	252	12	0.249	11	0.153	13	0.164	30	0.208
	$2^7$	504	12	0.444	13	0.388	13	0.247	35	0.445

**Example 3.** This example is taken from [41], with  $\Omega = [0, 2] \times [0, 2]$ . The diffusion coefficients are

$$c(x, y) = 1, \quad e(x, y) = 1 + xy, \quad (5.13)$$

and the source term is built from the exact solution given as

$$u(x, y) = x^4(2-x)^4y^4(2-y)^4. \quad (5.14)$$

Due to the nonsymmetry of the coefficient matrix caused by diffusion coefficients, the CG method has been replaced with GMRES. Nevertheless, the numerical results in Table 3 are comparable to those in Table 2. Indeed, the  $\tau$  preconditioner remains the best option, and the geometric multigrid preconditioner provides a good and robust alternative, especially when the problem is isotropic, i.e., when  $\alpha \approx \beta$ , also when applied to the band approximation.

## 6 Application to image deblurring

Fractional differential operators have been investigated to enhance diffusion in image denoising and deblurring [42, 43, 44]. In this section, we investigate the effectiveness of the previous preconditioning strategies to the Tikhonov regularization problem

$$\min_{\mathbf{u} \in \mathbb{R}^M} \|B_M \mathbf{u} - \mathbf{m}\|_2^2 + \mu \mathbf{u}^T A_M^{(\alpha, \beta)} \mathbf{u}, \quad (6.1)$$

where  $\mathbf{m}$  is the noisy and blurred observed image,  $B_M$  is the discrete convolution operator associated with the blurring phenomenon, and  $\mu > 0$  is the regularization parameter.

The solution of the least square problem (6.1) can be obtained by solving the linear system

$$\left( B_M^T B_M + \mu A_M^{(\alpha, \beta)} \right) \mathbf{u} = \mathbf{m}, \quad (6.2)$$

by the preconditioned CG method since the coefficient matrix is positive definite. The matrix  $B_M$  exhibits a block Toeplitz with Toeplitz blocks structure as the matrix  $A_M^{(\alpha, \beta)}$ , but the spectral behavior is completely

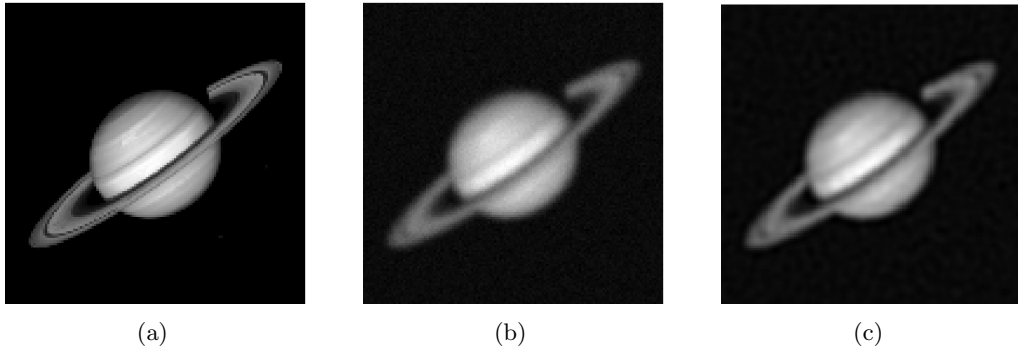


Figure 7: Image deblurring example: (a) true image, (b) observed image, (c) restored image for  $\mu = 10^{-4}$ .

Table 4: Image deblurring example: number of iterations and relative restoration error (RRE) for different values of  $\mu$ .

$\mu$	CG	$P_\tau$	$P_S$	RRE
$10^{-3}$	12	3	12	1.54e-01
$10^{-4}$	15	4	9	1.12e-01
$10^{-5}$	36	6	16	1.15e-01
$10^{-6}$	93	10	44	2.21e-01

different since the ill-conditioned subspace is very large and intersects substantially the high frequencies. Therefore, applying multigrid methods is quite challenging, see [45], and requires further investigation in the future. Here, we show the effectiveness of the  $\tau$  preconditioner in comparison with the Strang circulant preconditioner.

We consider the true satellite image of  $128 \times 128$  pixels in Figure 7 (a). The observed image in Figure 7 (b) is affected by a Gaussian blur and 5% of white Gaussian noise. We choose the fractional derivative  $\alpha = \beta = 1.1$  and the diffusion coefficients  $c(x, y) = e(x, y) = 1$ . The matrix  $A_M^{(\alpha, \beta)}$  is defined as in (5.5), while the Strang circulant and the  $\tau$  preconditioners are defined in (5.7) and (5.11), respectively. Since the quality of the reconstruction depends on the model (6.1), all the different solvers provide a similar reconstruction. The reconstructed image for  $\mu = 10^{-4}$  is shown in Figure 7 (c).

Various strategies exist for estimating the parameter  $\mu$ , see e.g. [46], but such estimation is beyond the scope of this work. Instead, we test different values of  $\mu$ . The linear system (6.1) is solved using the built-in *pcg* Matlab function with a tolerance of  $10^{-6}$ . Table 4 reports the number of iterations and the related restoration error for various values of  $\mu$ . It is noteworthy that the  $\tau$  preconditioner demonstrates a significant speedup compared to both CG without preconditioning and PCG with the Strang circulant preconditioner for all relevant values of  $\mu \in [10^{-5}, 10^{-3}]$ .

We should also point out that the considered images show a black background and hence all the various BCs are equivalent in terms of the precision of the reconstruction. However, in a general setting, we observe that the most precise BCs are related to the  $\tau$  algebra (see [25, 26] and references therein).

## 7 Conclusions

We discussed the convergence analysis of the multigrid method applied to a Riesz problem and compared it with state-of-the-art techniques. Associated numerical experiments highlight that  $\tau$  preconditioning is the best performing method. An application of the latter to an image deblurring problem with Tikhonov regularization

is given. This specific application will be considered in future research works, especially considering numerical methods for nonlinear models that require solving a linear problem as an inner step, see e.g. [47].

## Acknowledgements

The work of the authors is supported by the GNCS-INdAM project CUP E53C22001930001 and project CUPE53C23001670001. The work of the second author is partially funded by MUR – PRIN 2022, grant number 2022ANC8HL. The third author acknowledges the MUR Excellence Department Project MatMod@TOV awarded to the Department of Mathematics, University of Rome Tor Vergata, CUP E83C23000330006. The work of the fourth author is funded by the European High-Performance Computing Joint Undertaking (JU) under grant agreement No 955701. The JU receives support from the European Union’s Horizon 2020 research and innovation program and Belgium, France, Germany, and Switzerland. Furthermore, the fourth is grateful for the support of the Laboratory of Theory, Economics and Systems – Department of Computer Science at Athens University of Economics and Business.

## References

- [1] Anshima Singh, Sunil Kumar, and Jesus Vigo-Aguiar. High-order schemes and their error analysis for generalized variable coefficients fractional reaction–diffusion equations. Mathematical Methods in the Applied Sciences, 46(16):16521–16541, 2023.
- [2] Mariarosa Mazza, Marco Donatelli, Carla Manni, and Hendrik Speleers. On the matrices in B-spline collocation methods for Riesz fractional equations and their spectral properties. Numerical Linear Algebra with Applications, 30(1):e2462, 2023.
- [3] Mark M Meerschaert and Charles Tadjeran. Finite difference approximations for fractional advection–dispersion flow equations. Journal of computational and applied mathematics, 172(1):65–77, 2004.
- [4] Tian-Yi Li, Fang Chen, Hai-Wei Sun, and Tao Sun. Preconditioning technique based on sine transformation for nonlocal Helmholtz equations with fractional Laplacian. Journal of Scientific Computing, 97(1):17, 2023.
- [5] Carlo Garoni and Stefano Serra-Capizzano. Generalized locally Toeplitz sequences: theory and applications, volume 1. Springer, 2017.
- [6] Carlo Garoni, Hendrik Speleers, Sven-Erik Ekström, Alessandro Reali, Stefano Serra-Capizzano, and Thomas JR Hughes. Symbol-based analysis of finite element and isogeometric B-spline discretizations of eigenvalue problems: Exposition and review. Archives of Computational Methods in Engineering, 26(5):1639–1690, 2019.
- [7] Marco Donatelli, Mariarosa Mazza, and Stefano Serra-Capizzano. Spectral analysis and structure preserving preconditioners for fractional diffusion equations. Journal of Computational Physics, 307:262–279, 2016.
- [8] Marco Donatelli, Rolf Krause, Mariarosa Mazza, and Ken Trotti. Multigrid preconditioners for anisotropic space-fractional diffusion equations. Advances in Computational Mathematics, 46(3):1–31, 2020.
- [9] Siu-Long Lei and Hai-Wei Sun. A circulant preconditioner for fractional diffusion equations. Journal of Computational Physics, 242:715–725, 2013.
- [10] Xin Huang, Xue-Lei Lin, Michael K. Ng, and Hai-Wei Sun. Spectral analysis for preconditioning of multi-dimensional Riesz fractional diffusion equations. Numerical Mathematics: Theory, Methods and Applications, 15(3):565–591, 2022.

- [11] Nikos Barakitis, Sven-Erik Ekström, and Paris Vassalos. Preconditioners for fractional diffusion equations based on the spectral symbol. Numerical Linear Algebra with Applications, page e2441, 2022.
- [12] Stefano Serra-Capizzano and Eugene E Tyrtshnikov. Any circulant-like preconditioner for multilevel matrices is not superlinear. SIAM Journal on Matrix Analysis and Applications, 21(2):431–439, 2000.
- [13] Lidia Aceto and Mariarosa Mazza. A rational preconditioner for multi-dimensional Riesz fractional diffusion equations. Computers & Mathematics with Applications, 143:372–382, 2023.
- [14] Hong-Kui Pang and Hai-Wei Sun. Multigrid method for fractional diffusion equations. Journal of Computational Physics, 231(2):693–703, 2012.
- [15] Hamid Moghaderi, Mehdi Dehghan, Marco Donatelli, and Mariarosa Mazza. Spectral analysis and multigrid preconditioners for two-dimensional space-fractional diffusion equations. Journal of Computational Physics, 350:992–1011, 2017.
- [16] Marco Donatelli, Mariarosa Mazza, and Stefano Serra-Capizzano. Spectral analysis and multigrid methods for finite volume approximations of space-fractional diffusion equations. SIAM Journal on Scientific Computing, 40(6):A4007–A4039, 2018.
- [17] Mark M Meerschaert and Charles Tadjeran. Finite difference approximations for two-sided space-fractional partial differential equations. Applied numerical mathematics, 56(1):80–90, 2006.
- [18] Hong Wang, Kaixin Wang, and Treena Sircar. A direct  $O(N \log^2 N)$  finite difference method for fractional diffusion equations. Journal of Computational Physics, 229(21):8095–8104, 2010.
- [19] Hong-Kui Pang and Hai-Wei Sun. Fast numerical contour integral method for fractional diffusion equations. Journal of Scientific Computing, 66(1):41–66, 2016.
- [20] Stefano Serra-Capizzano. On the extreme spectral properties of Toeplitz matrices generated by L1 functions with several minima/maxima. BIT, 36(1):135–142, 1996.
- [21] Stefano Serra-Capizzano. On the extreme eigenvalues of Hermitian (block) Toeplitz matrices. Linear algebra and its applications, 270(1-3):109–129, 1998.
- [22] Albrecht Böttcher and Sergei M Grudsky. On the condition numbers of large semidefinite Toeplitz matrices. Linear algebra and its applications, 279(1-3):285–301, 1998.
- [23] Owe Axelsson and Gunhild Lindskog. On the rate of convergence of the preconditioned conjugate gradient method. Numerische Mathematik, 48(5):499–523, 1986.
- [24] Stefano Serra-Capizzano. Toeplitz preconditioners constructed from linear approximation processes. SIAM Journal on Matrix Analysis and Applications, 20(2):446–465, 1998.
- [25] Stefano Serra-Capizzano. A note on antireflective boundary conditions and fast deblurring models. SIAM Journal on Scientific Computing, 25(4):1307–1325, 2004.
- [26] Marco Donatelli and Stefano Serra-Capizzano. Anti-reflective boundary conditions and re-blurring. Inverse Problems, 21(1):169, 2004.
- [27] Marco Donatelli, Carlo Garoni, Carla Manni, Stefano Serra-Capizzano, and Hendrik Speleers. Robust and optimal multi-iterative techniques for IgA Galerkin linear systems. Computer Methods in Applied Mechanics and Engineering, 284:230–264, 2015.
- [28] John W Ruge and Klaus Stüben. Algebraic multigrid. In Multigrid methods, pages 73–130. SIAM, 1987.
- [29] Ulrich Trottenberg, Cornelius W Oosterlee, and Anton Schuller. Multigrid. Elsevier, 2000.

- [30] Giuseppe Fiorentino and Stefano Serra-Capizzano. Multigrid methods for symmetric positive definite block Toeplitz matrices with nonnegative generating functions. SIAM Journal on Scientific Computing, 17(5):1068–1081, 1996.
- [31] Raymond H Chan, Qian-Shun Chang, and Hai-Wei Sun. Multigrid method for ill-conditioned symmetric Toeplitz systems. SIAM Journal on Scientific Computing, 19(2):516–529, 1998.
- [32] Antonio Aricò and Marco Donatelli. A V-cycle multigrid for multilevel matrix algebras: proof of optimality. Numerische Mathematik, 105(4):511–547, 2007.
- [33] Marco Donatelli. An algebraic generalization of local Fourier analysis for grid transfer operators in multigrid based on Toeplitz matrices. Numerical Linear Algebra with Applications, 17(2-3):179–197, 2010.
- [34] Giuseppe Fiorentino and S Serra-Capizzano. Multigrid methods for Toeplitz matrices. Calcolo, 28(3):283–305, 1991.
- [35] Antonio Aricò, Marco Donatelli, and Stefano Serra-Capizzano. V-cycle optimal convergence for certain (multilevel) structured linear systems. SIAM Journal on Matrix Analysis and Applications, 26(1):186–214, 2004.
- [36] Stefano Serra-Capizzano. Convergence analysis of two-grid methods for elliptic Toeplitz and PDEs matrix-sequences. Numerische mathematik, 92(3):433–465, 2002.
- [37] Danyal Ahmad, Marco Donatelli, Mariarosa Mazza, S Serra-Capizzano, and Ken Trotti. A smoothing analysis for multigrid methods applied to tempered fractional problems. Linear and Multilinear Algebra, pages 1–24, 2023.
- [38] Stefano Serra-Capizzano. An ergodic theorem for classes of preconditioned matrices. Linear Algebra and its Applications, 282(1-3):161–183, 1998.
- [39] Tony F Chan. An optimal circulant preconditioner for Toeplitz systems. SIAM journal on scientific and statistical computing, 9(4):766–771, 1988.
- [40] Dario Bini and Milvio Capovani. Spectral and computational properties of band symmetric Toeplitz matrices. Linear Algebra and its Applications, 52:99–126, 1983.
- [41] Kejia Pan, Hai-Wei Sun, Yuan Xu, and Yufeng Xu. An efficient multigrid solver for two-dimensional spatial fractional diffusion equations with variable coefficients. Applied Mathematics and Computation, 402:126091, 2021.
- [42] Qi Yang, Dali Chen, Tiebiao Zhao, and YangQuan Chen. Fractional calculus in image processing: a review. Fractional Calculus and Applied Analysis, 19(5):1222–1249, 2016.
- [43] Harbir Antil and Sören Bartels. Spectral approximation of fractional PDEs in image processing and phase field modeling. Computational Methods in Applied Mathematics, 17(4):661–678, 2017.
- [44] Stefano Aleotti, Alessandro Buccini, and Marco Donatelli. Fractional graph Laplacian for image reconstruction. Applied Numerical Mathematics, 2023.
- [45] Marco Donatelli. A multigrid for image deblurring with Tikhonov regularization. Numerical linear algebra with applications, 12(8):715–729, 2005.
- [46] Per Christian Hansen. Rank-deficient and discrete ill-posed problems: numerical aspects of linear inversion. SIAM, 1998.
- [47] Yuantao Cai, Marco Donatelli, Davide Bianchi, and Ting-Zhu Huang. Regularization preconditioners for frame-based image deblurring with reduced boundary artifacts. SIAM Journal on Scientific Computing, 38(1):B164–B189, 2016.